

Ionospheric Plasma Drift and Neutral Winds Modeling

Chapagain N.P.

Patan Multiple Campus, Patan Dhoka, Lalitpur, Tribhuvan University, Nepal
npchapagain@gmail.com

Available online at: www.isca.in, www.isca.me

Received 16th July 2016, revised 8th August 2016, accepted 2nd September 2016

Abstract

This study reports the modeling results of the ionospheric plasma drift zonal velocity and the neutral wind motions. To determine zonal plasma drift velocity, we use theoretical formulations for ionospheric vertical electric field responsible for the development of the zonal plasma drift velocity. We obtain the modeling results of the neutral wind motions using the Horizontal wind models (HWM093 and HWM07). The computed drift velocity is also compared with the experimental results of neutral winds motions measured by the Febry Perot Interferometer. In addition, the equatorial plasma bubbles (EPBs) velocities as measured by OI airglow optical imaging system are also used to compare with the model results of ionospheric plasma drifts and neutral wind motions. Results show that trend of variations of model results of plasma drift velocity and local wind motions are similar, while the magnitude of EPBs drifts velocity most often shows quiet different values. Furthermore, the model results for the plasma drift velocity and the neutral wind motions obtained from HWM93 illustrate good agreement with the experimental results of neutral winds and EPBs velocity as compared with the model results derived from HWM07.

Keywords: Plasma drift, Neutral winds, HWM093, HWM07, Equatorial plasma bubbles.

Introduction

The dynamics of the upper atmosphere of the Earth is primarily affected by phenomena by radiative, chemical, thermal and neutral atmospheric and plasma transport. The previous studies of Ionospheric and thermospheric phenomena have been carried out using theoretical as well as experimental set up such as ground-based and in-situ measurements of electron density and temperature, ion temperatures and composition, and plasma velocity. Similarly, the dynamics of the low-latitude ionosphere have been studied with the radars, ionosondes, magnetometers, and spaced-based techniques^{1,2}. Using both ground- and satellite-based observations, the widespread investigations of equatorial and low latitude plasma drifts have been performed in several studies^{1,3-5}. Besides theoretical and numerical modeling studies, coincident radar and optical measurements were being used to estimate the zonal plasma drifts and to study thermosphere-ionosphere coupling⁶⁻⁹. Similarly, satellite observations have also been used to find the spatial variations of plasma drifts velocity. The characteristics of plasma drifts and electric fields were reported mainly by the radar observations from Jicamarca Radio Observatory (JRO), Peru (11.9°S, 76.8°W)¹⁰.

In the past few years, many empirical as well as theoretical simulations have been formulated for the clarification of climatology of the global ionosphere-thermosphere. Meriwether et al.¹¹ reported climatology of thermospheric neutral winds and temperatures from Fabry-Perot interferometer measurements. Understanding the behavior of the equatorial thermospheric

wind is key to understanding the physics of the F-region dynamo¹²⁻¹⁴. Chapagain et al.⁹ described the comparison of zonal neutral wind motions with the equatorial plasma bubbles (EPBs) drift velocity measured by airglow emission from Brazil. They investigated that the EPBs drift velocity are similar to the background motions of ionospheric plasma drift and hence with the neutral winds motions¹⁵.

In this study, we have computed ambient ionospheric plasma drift velocity using theoretical formulations for vertical electric field responsible for the development of the zonal plasma drifts. For such computation, we have used Horizontal wind models and ionospheric conductivities as briefly discussed below. The computed ionospheric plasma drifts are also compared to experimental results of neutral wind motions measured by the Febry Perot Interferometer and theoretical model of the neutral winds obtained from horizontal wind models. We also use the equatorial plasma bubble (EPBs) velocities as measured by optical imaging system to compare with ionospheric plasma drifts modeling.

Horizontal Wind Model: The Horizontal Wind Model 1993 (HWM093) is an empirical model developed for the zonal neutral wind in upper thermosphere using data derived from the AE-E (Atmospheric Explorer E) and DE-2 satellites¹⁶. Similarly, Horizontal Wind Model 1990 (HWM90) was extended down to 100 km using wind data obtained from incoherent scatter radar (ISR) and Fabry-Perot optical interferometers, while HWM93 was further extended down to the ground using MF/Meteor data. These wind models software

also specify the zonal as well as meridional winds for particular locations such as latitude, longitude and time. Horizontal Wind Model 2007 (HWM07) plays a vital role to investigate the low latitude ionospheric dynamics¹⁷.

Ionospheric Conductivity: The dynamics of the upper atmosphere are primarily controlled by solar heating tidal forces. Solar radiation sets up a global system of neutral winds on the day-side that tend to flow toward the colder regions on the night-side. As these neutral winds drive ionospheric plasma across magnetic field lines, electric fields are generated. This plays significant role in the distribution of ionization. On the other hand, collisions between neutral atmosphere and ions, ions and electrons, and the neutrals and electrons are the cause of the conductivity in the ionosphere¹⁸.

The ionospheric conductivity has a major role in F-region electrodynamics. These conductivities constituents: Pedersen, Hall, and parallel conductivity¹⁸. The conductivity parallel to the electric field, but perpendicular to magnetic field, is called Pederson conductivity. The conductivity perpendicular to both the electric and magnetic fields is called Hall conductivity, while the conductivity parallel to the magnetic field alone is defined as parallel conductivity. In model calculations of the ionospheric plasma drift, we have used the Pederson and Hall conductivity.

Theory: The ambient ionospheric plasma drift velocities were determined from theoretical simulations for ionospheric vertical electric field responsible for development of plasma drifts^{6,19,21}. To estimate zonal drift velocities, following mathematical relations are used.

The local Pedersen conductivity (σ_p) and Hall conductivity (σ_H) can be expressed by the relations¹⁸.

$$\sigma_p = \frac{qN_e}{B} \left[\frac{|k_e|}{1+k_e^2} + \frac{k_i}{1+k_i^2} \right] \quad (1)$$

$$\sigma_H = \frac{qN_e}{B} \left[\frac{k_e^2}{1+k_e^2} - \frac{k_i^2}{1+k_i^2} \right] \quad (2)$$

Here: q is charges of ions; N_e is electron density number, k_e is mobility of electron and k_i is mobility of ions. These can be given by:

$$k_e = \omega_e / \vartheta_{en} \quad \text{and} \quad k_i = \omega_i / \vartheta_{in} \quad (3)$$

Here, ω_e and ω_i are electron and ion gyrofrequencies, ϑ_{en} is electron-to-neutral collision frequency and ϑ_{in} is ion-to-neutral collision frequency, which are calculated similar to explained by Sobralet al.²¹.

Field line integrated Pedersen conductivity (Σ_p) and hall conductivity (Σ_H) were calculated on the process of integration along the geomagnetic field lines using International

Geomagnetic Reference Field (IGRF) trace field model. We further estimated the Pedersen conductivity (U_ϕ^p) and hall conductivity (U_L^H) weighted winds by applying the field-line integral as expressed as followings:

$$U_\phi^p = \frac{1}{\Sigma_p} \int_{ha}^{ht} \sigma_p u_z dr \quad (4)$$

$$U_L^H = \frac{1}{\Sigma_H} \int_{ha}^{ht} \sigma_p u_q dr \quad (5)$$

Here, ht is the target lower limit of altitude (90 km) and ha is apex altitude (250 km). The step size of 1 km height is integrated. Here: u_z denotes local zonal wind motion at a particular place in geomagnetic coordinate, and u_q represents the local vertical meridional wind motion in the magnetic meridional plane and perpendicular to magnetic field lines. The integrated Pedersen and hall conductivities were calculated from both E- and F-region ionosphere. To determine the zonal plasma drift speed (v_z), we used the following relation as reported by Sobralet al.²¹.

The zonal plasma drifts velocity, $v_z = \frac{E_q}{B}$

$$v_z = \left\{ U_\phi^p - \frac{\Sigma_H}{\Sigma_p} (V_l - U_L^H) \right\} \frac{(1+3\zeta^2)^{1/2}}{(1-\zeta^2)^{3/2}} \quad (6)$$

here, E_q is the vertical electric field at geomagnetic latitude λ and B denotes the Earth's magnetic field intensity, V_l represents the vertical drift speed at geomagnetic equator, and $\zeta = \sin\lambda$, ($\lambda = 6^\circ$ S at Cajazeiras, Brazil).

Methodology

The plasma zonal drift speed is determined using theoretical simulations of vertical electric field in the ionosphere, which is responsible for development of ionospheric zonal plasma drifts as derived above in equations (6). We also use the HWM93¹⁶ and HWM0717. Similarly, NRLMSIS-00 model (Naval Research Laboratory Mass Spectrometer and Incoherent Scatter Radar)²² has been applied to derive the densities of neutral species of O_2 , N_2 , O, and N.

Furthermore, the empirical ionospheric IRI-2007 (International Reference Ionosphere) model^{23,24} has been used to derive electron density (N_e) and ion density (N_i) of the species such as O_2 , N_2 , O and N, and electron temperature (T_e). IGRF (International Geomagnetic Reference Field) traced field model has been used for the determination of integrated Pedersen and hall conductivities. The vertical plasma drift speed has been derived from Scherliess and Fejer empirical model²⁵. We used Matlab programming code to develop the algorithm for the derivation of these data. We used the equation (6) to estimate zonal plasma drift speed using Matlab coding and values of corresponding variables were also estimated using the equations (1) to (5).

The detail of experimental set up to measure the neutral winds motions by using Fabry Perot Interferometer and equatorial plasma bubble (EPBs) drifts speeds measured by optical imaging system is explained in detail by Chapagain et al.⁹. Since we have the experimental set up for the zonal wind measurements and EPBs drift velocities near geomagnetic equator from South America, Brazil, the model results of neutral winds motion and plasma drift speeds were also estimated from the same locations for the comparative studies.

Results and Discussion

We have computed the theoretical ambient plasma drift velocity using the equation (6) as derived above. For the computation of the plasma drift, we use both HWM93 and HWM07 models. These models are also used to derive neutral wind motions to compare with experimental results of zonal neutral winds motions and EPBs drift speeds.

Figure-1 (in top-panel) plots the comparison of the model results for the local zonal winds (indicated by dash-dash line with sky blue color), Pedersen conductivity weighed wind motions (denoted by solid blue line) obtained from HWM93, and experimental results of neutral winds motion (represented by the solid line with vertical bars with green line) on October 20, 2009. The positive values in the plot represent the eastward motions, while the negative values are the westward motions. Here the time is expressed in universal time (UT) in which the local time lags behind by 2 hours (i.e. LT = UT-2). The model results of local winds and Pedersen conductivity weighted wind motions nearly match with our wind measurements around 01:00 UT, 04:15 UT and 06:30 UT. While in the early evening hours (before ~23:00 UT), the model results are significantly larger than the observed wind motions. Moreover, our results show the westward reversal of wind motions after ~02:30 UT, whereas the model wind motions continue in the eastward direction.

The plot of the bottom panel of Figure-1 compares the plasma drift models (solid black line) and model results of the neutral winds with the experimental results of EPBs (scatter plots in circles). Trend of variations of model results of plasma drift velocity and local wind motions are similar pattern, while the magnitude of EPB drifts velocity are quite different. The model results of plasma drifts and neutral winds show similar pattern throughout the night. The plasma drifts, neutral winds, and EPBs velocities, all are in eastward and increase in magnitude as time progresses in the early evening hour, while around the mid-night and post-midnight hours, the velocities decreases with time progresses.

Figure-2 in the top panel plots the experimental results of the zonal neutral wind motions, the weighted wind model and local wind models obtained from horizontal wind model 2007 (HWM07) during same night (20 October 2009) as plotted in Figure-1.

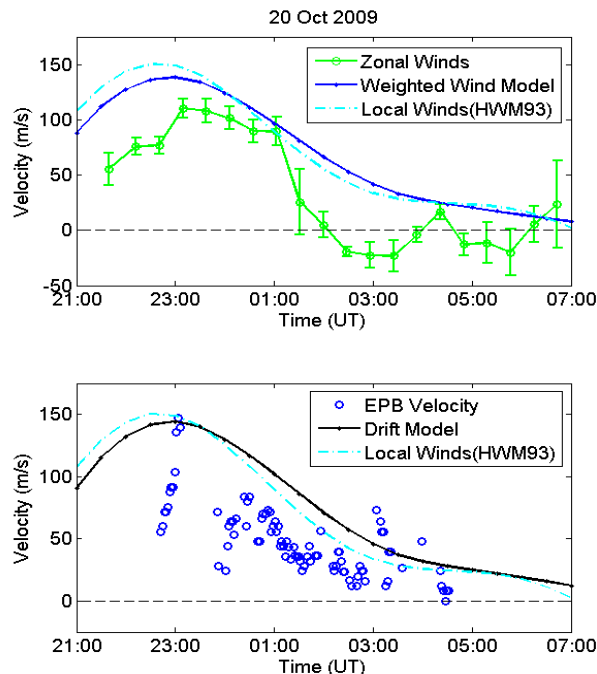


Figure-1
 Comparisons of the model results of the zonal neutral wind motions using HWM93 with the experimental results of neutral winds (top panel) and the EPBs drift velocity and zonal plasma drift model (bottom panel) on 20 October 2009

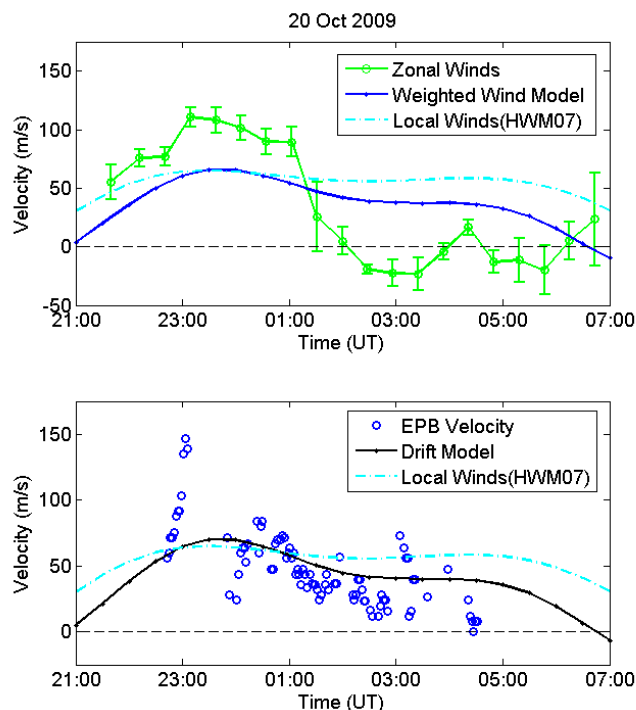


Figure-2
 Comparisons of the model results of the zonal neutral wind motions using HWM07 with the experimental results of neutral winds (top panel) and EPBs drift speed and zonal plasma drift model (bottom panel) on 20 October 2009

Similarly, the bottom panel of Figure-2 shows comparison EPBs velocities, computed results of the plasma drift model, and local zonal winds model from HWM07. These models do not follow the actual trends of the nighttime variations of the wind measurements and plasma drift velocities as reported by the previous investigations^{5,10}.

The model results for the plasma drift velocity and the local wind motions obtained from HWM93 (Figure-1) show the better match with the experimental results of neutral winds and EPBs velocity as compared with the model results derived from HWM07 (Figure-2). Therefore, we use the HWM93 model results for the further comparisons with the experimental results.

Figure-3 shows the comparisons between the experimental and model results of zonal neutral winds motions using HWM93, ionospheric plasma drift model, and EPBs drift velocities on November 8, 2009 and December 17, 2009. On November 8, the results show the trend of variations of the model results nearly consistent with the experimental results of neutral winds and the EPBs drift speeds. However, the magnitudes of model results of both neutral winds motions and plasma drifts velocities show quiet larger than the observations results of winds motions and EPB drift velocity. In contrast, on December 17, the experimental results of neutral wind motions are significantly larger than the model results during the time period of 23:00-01:00 UT with differences of peak value up to 60 m/s. Experimental results of neutral wind motions also exceed the model results after ~ 04:00 UT till the dawn. However, results of plasma drift model are nearly agreement with the EPBs drift velocities.

Figure-4 compares the model results of plasma drift velocities with the experimental results of neutral winds motions and EPBs drift speeds on November 5 and December 5, 2010. On November 5, there is a good consistent in the variations of wind motions with plasma drifts model results and EPBs drifts velocity during the period of ~ 23:00-04:00 UT. However, in the early evening hours, (before 23:00 UT), the model results are larger than the observational results. Similarly, on December 5, the plots show the similar pattern of variations of model results with experimental results. The computed drifts velocities from these two nights are good consistent with the observations after ~23:00 UT, while before this hour, these values are larger than the measurement results.

Interestingly, our measurements show the westward reversal of winds on 20 October 2009, while the model results for the local winds and Pedersen conductivity weighted wind speeds from HWM93 and HWM07 shows eastward throughout the night. Sobral et al.²⁶ have reported that reversal to westward motion of EPBs around midnight is due to the reversal of the Pedersen conductivity weighted winds speeds. However, our measurements illustrate that the local winds can also exhibit the westward reversal around the local midnight and post-midnight hours. Such investigations of good consistent of local wind and EPBs velocity and late night reversal of plasma drift velocity and neutral winds motion were presented in previous studies by Sobral et al.²⁶ and Chapagain et al.⁹. Similarly, the early evening variations of neutral wind motions from plasma drifts velocity were also reported in the comparative studies of neutral wind motion and EPBs drift velocity by Chapagain et al.⁹.

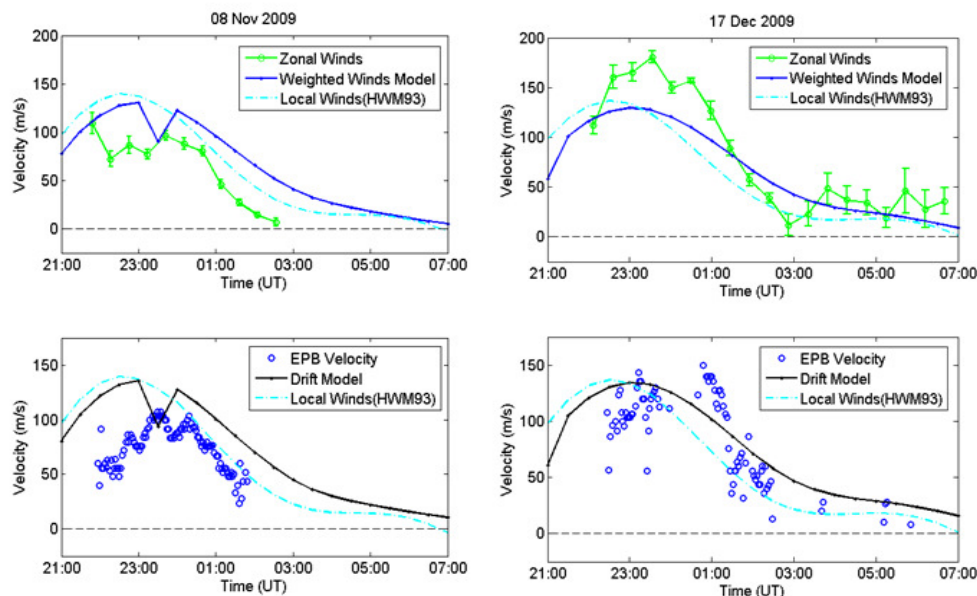


Figure-3

Comparisons of the model results of the zonal neutral wind motions using HWM93 with the experimental results of neutral winds (top panel) and the EPBs drifts velocity and plasma drifts model (bottom panel) on 8 November 2009 and 17 December 2009

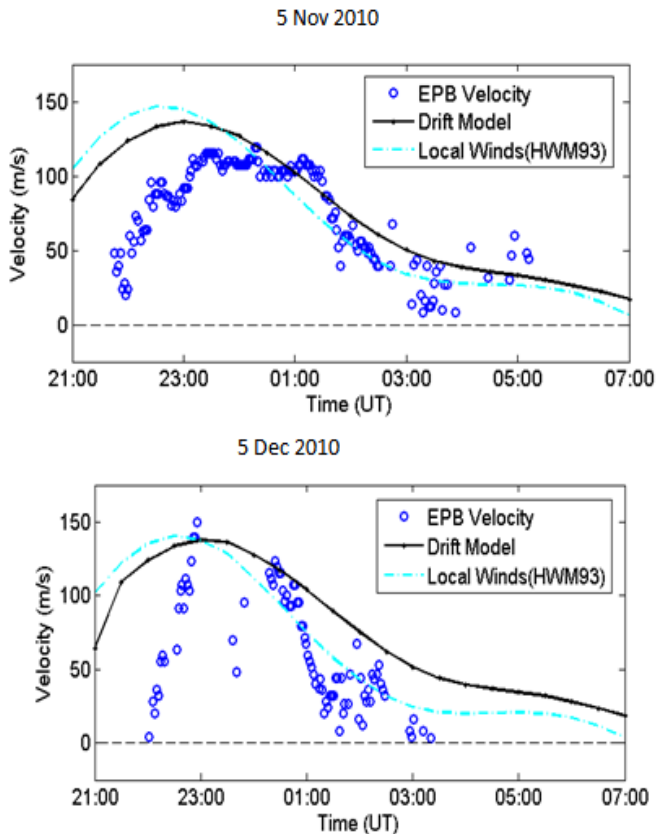


Figure-4

Comparisons of model results of the neutral wind motions using HWM93 with the plasma drift model and with experimental results of the EPBs drift velocity on 5 November and 5 December 2010

Conclusion

In this paper, ambient ionospheric plasma zonal drift velocity has been computed using theoretical simulations for ionospheric vertical electric field that develops zonal plasma drift velocity. For such computation, we have used horizontal wind models (HWM093 and HWM07), the empirical ionospheric IRI-2007 model, and NRLMSIS-00 model. The computed ionospheric ambient plasma drift velocities are compared with the experimental results of neutral winds motions measured by the Febry Perot Interferometer and the model results of the neutral winds motions obtained using HWM93 and HWM07 models from the same location. In addition, the EPBs velocities as measured using airglow all-sky digital images by optical imaging system are also compared with the model results of ionospheric plasma drift velocity.

Trend of variations of model results of plasma drift velocity and local wind motions are similar, while the EPBs drifts velocity show quite different in their magnitudes. The plasma drift velocities are in eastward in all nights which increase with time progresses in early evening hours while in around the mid-night

and post mid-night hours, the velocities decrease with time progresses. Furthermore, the simulation results of the plasma drift velocity and local wind motions obtained using HWM93 show the better consistent with the experimental results of neutral winds motion and plasma bubble drift velocity as compared with the model results derived from HWM07.

Acknowledgements

Author thanks Prof. Jonathan J. Makela, University of Illinois at Urbana-Champaign, Illinois, USA and Prof. John Meriwether from Clemson University, USA for providing the data from optical imaging systems and the FPI neutral winds measurements for the comparison with the model study. Author also thanks to Tim Duly for his assistant for development Matlab coding for simulation work.

References

1. Fejer B.G., J.R. Souza, A.S. Santos and A.E. Costa Pereira (2005). Climatology of F region zonal plasma drifts over Jicamarca. *J. Geophys. Res.*, 110, A12310, doi:10.1029/2005JA011324.
2. Chapagain N.P. (2015). Electrodynamics of the Low-latitude Thermosphere by Comparison of Zonal Neutral Winds and Equatorial Plasma Bubble Velocity. *Journal of Institute of Science and Technology*, Tribhuvan University, 20(2), 84-89.
3. de Paula E.R. et al (2002). Ionospheric irregularity zonal velocities over Cachoeira Paulista. *J. Atmos. Sol.-Terr. Phys.*, 64(12), 1511-1516.
4. Pautet P.D., M.J. Taylor, N.P. Chapagain, H. Takahashi, A.F. Medeiros, F.T. Sao Sabbas and D.C. Fritts (2009). Simultaneous observations of equatorial F-region plasma depletions over Brazil during the spread F Experiment (SpreadFEx). *Ann. Geophys.*, 27, 2371-2381.
5. Chapagain N.P., M.J. Taylor, J.J. Makela and T.M. Duly (2012). Equatorial plasma bubble zonal velocity using 630.0 nm airglow observations and plasma drift modeling over Ascension Island. *J. Geophys. Res.*, 117, A06316, doi: 10.1029/2012JA 017750.
6. Haerendel, G., J.V. Eccles and S. Cakir. (1992). Theory for modeling the equatorial evening ionosphere and the origin of the shear in the horizontal plasma flow. *J. Geophys. Res.*, 97(A2), 1209-1223, doi: 10.1029/91JA02226.
7. Richmond A.D, E.C. Ridley and R.G. Roble. (1992). A Thermosphere/Ionosphere general circulation model with coupled electrodynamics. *Geophys. Res. Lett.*, 9, 601-604.
8. Chapagain N.P., M.J. Taylor and J.V. Eccles. (2011). Airglow observations and modeling of F region depletion zonal velocities over Christmas Island. *J. Geophys. Res.*, 116, A02301, doi: 10.1029/2010JA015958.

9. Chapagain N.P., J.J. Makela, J.W. Meriwether, D.J. Fisher, R.A. Buriti and A.F. Medeiros. (2012). Comparison of Nighttime Zonal Neutral Winds and Equatorial Plasma Bubble Drift Velocities over Brazil. *J. Geophys. Res.*, 117, A06309. doi: 10.1029/2012JA017620.
10. Fejer B.G., E.R. de Paula, S.A. Gonzalez and R.F. Woodman (1991). Average vertical and zonal F region plasma drifts over Jicamarca. *J. Geophys. Res.*, 96(A8), 13, 901-13, 906, doi: 10.1029/91JA01171.
11. Meriwether JW, J.J. Makela, Y. Huang, D.J. Fisher, R.A. Buriti, A.F. Medeiros and H Takahashi (2011). Climatology of the nighttime equatorial thermospheric winds and temperatures over Brazil near solar minimum. *J. Geophys Res*, 116, A04322, doi: 10.1029/2011JA016477.
12. Rishbeth H. (1971). Polarization fields produced by winds in the equatorial F-region. *Planet. Space Sci.*, 19, 357-369.
13. Heelis R.A., P.C. Kendall, R.J. Moffet, D.W. Windle and H. Rishbeth (1974). Electrical coupling of the E and F-regions and its effect on the F-region drifts and winds. *Planet. Space Sci.*, 22, 743-756.
14. Immel T.J., H.U. Frey, S.B. Mende and E. Sagawa (2004). Global observations of the zonal drifts speed of equatorial ionospheric plasma bubbles. *Ann. Geophys.*, 22, 3099-3107.
15. Rishbeth H. (1997). The ionospheric E-layer and F-layer dynamos -a tutorial review. *Journal of Atmospheric and Solar-Terrestrial Physics*, 59, 1873-1880.
16. Hedin A., E.L. Fleming, A.H. Manson, F.J. Schmidlin, S.K. Avery, R.R. Clark, S.J. Franke, G.J. Frasier, T. Tsuda, F. Vial and R.A. Vincent. (1996). Empirical wind model for the upper, middle and lower atmosphere. *J. Atmos. Terr. Phys.*, 58, 1421-1447.
17. Drob D.P. et al. (2008). An empirical model of the Earth's horizontal wind fields: HWM07. *J. Geophys. Res.*, 113, A12304, doi: 10.1029/2008JA013668.
18. Kelley M.C. (2009). The Earth's Ionosphere: Plasma physics and electrodynamics, second edition. Academic Press, San Diego, California.
19. Eccles J.V. (1998). A simple model of low-latitude electric fields. *J. Geophys. Res.*, 103(A11), 26699-26708.
20. Eccles J.V., N. Maynard and G. Wilson. (1999). Study of the evening plasma drift vortex in the low-latitude ionosphere using San Marco electric field measurements. *J. Geophys. Res.*, 104(A12), 28133-28143.
21. Sobral J. H. A. et al. (2009). Ionospheric zonal velocities at conjugate points over Brazil during the COPEX campaign: experimental observations and theoretical validations. *J. Geophys. Res.*, 114, A04309, doi: 10.1029/2008JA013896.
22. Picone J.M., A.E. Hedin, D.P. Drob and A.C. Aikin. (2002). NRLMSISE-00 empirical model of the atmosphere: Statistical comparisons and scientific issues. *J. Geophys. Res.*, 107(A12), 1468, doi: 10.1029/2002JA009430.
23. Bilitza D. et. al. (1990). International Reference Ionosphere. NSSDC 90-22, Greenbelt, Maryland.
24. Bilitza D. and B. Reinisch (2008). International Reference Ionosphere 2007: Improvements and new parameters. *J. Adv. Space Res.*, 42(4), 599-609, doi:10.1016/j.asr.2007.07.048.
25. Scherliess L. and B. G. Fejer (1999). Radar and satellite global equatorial F-region vertical drift model. *J. Geophys. Res.*, 104, 6829-6842.